A Learning-Based Approach for Automatic Defect Detection in Textile Images

Daniel Yapi, **Marouene Mejri**, **Mohand Saïd Allili**, **Nadia Baaziz**

Département d'informatique et d'ingénierie, Université du Québec en Outaouais. Pavillon Lucien Brault, J8X 3X7, Gatineau, QC, Canada.
E-mails: {ndahdaniel.yapi, mohandsaid.allili, nadia.baaziz, marouene.mejri}@ uqo.ca.

Abstract: This paper addresses the textile defect detection problem using a machine-learning approach. We propose a novel algorithm that uses supervised learning to classify textile textures in defect and non-defect classes based on suitable feature extraction and classification. We use statistical modeling of multi-scale contourlet image decomposition to obtain compact and accurate signatures for texture description. Our defect detection algorithm is based on two phases. In the first phase, using a training set of images, we extract reference defect-free signatures for each textile category. Then, we use the Bayes classifier (BC) to learn signatures of defected and non-defected classes. In the second phase, defects are detected on new images using the trained BC and an appropriate decomposition of images into blocks. Our algorithm has the capability to achieve highly accurate defect detection and localisation in textile textures while ensuring an efficient computational time. Compared to recent state-of-the-art methods, our algorithm has yielded better results on the standard TILDA database.

Keywords: Textile defect detection, mixtures of generalized Gaussians (MoGG), contourlets, Bayes classifier.

1. INTRODUCTION

Automatic product inspection is a major concern in quality control of various industrial products. Textile industry is one of the biggest traditional industries where automated inspection systems play a critical role in reducing inspection time and increasing production rate. Textile is used in multiple products such as clothing, filters, cloths, wipes, and in housing and transportation materials. During the process of knitting a textile fabric frame, several types of defects may occur. For instance, the yarn used can be cut then resulting in a gap in the frame, a stain of oil can be caused by the knitting device or a color difference can be marked during the cloth drying (see Fig. 1 for illustration). Typical textile fabrics are 13 meters wide and are driven with speeds ranging from 20 to 200 meters/min (Cho et al. (2005); Kumar (2008)). Thus, manual defect detection done by experts becomes quickly an overwhelming and fastidious task. Therefore, having efficient and automatic inspection systems at hand is a major requirement for improving reliability and speeding up the quality control, which may increase the productivity.

The topic of automatic defect detection has been investigated in several works in the last decades. Although there is no universal approach for tackling this problem, several methods based on image processing techniques have been proposed in recent years (see recent surveys Cho et al. (2005); Kumar (2008); Ngana et al. (2011)). These methods rely mainly on analysing texture images for detecting potential patterns that differ from the main defect-free texture. These approaches can be classified into three main groups: *statistical*, *spectral* and *model-based* ones. Statistical approaches use gray-level texture features derived from co-occurrence matrices, or the local mean and standard deviation for detecting fabric defects. For instance, Cho et al. (2005) have proposed an approach for inspection which operates at the line level to detect defects in uniform textures. Tajeripour et al. (2008) have used local binary patters (LBP) for detecting defects in fabrics. In that work, a learning phase is carried out first by applying the LBP operator to an image of a defect-free fabric. Then, defects are detected in new images using an appropriate threshold. The applicability of these approaches is however limited to uniform (non-patterned) textures.

Spectral approaches consist mainly on locating defects in the spectral domain (Kumar (2008)). For instance, Chan and Pang (2000) have used Fourier analysis to locate defects in gray-level images. In the same vein, Kumar and Pang (2002) have used multichannel Gabor filters and supervised learning for detecting defects in textured materials. However, Gabor techniques need generally a large amount of computations, while an optimal fusion of different information channels remains an open issue. More recently, Ngan et al. (2005) have used the wavelet transform for detecting and locating defects in patterned textures. This method is capable of detecting defects for different types of textures. However, it uses adaptive thresholds which are fixed manually.

⋆ This work has been completed with the support of the Natural Sciences and Engineering Research Council of Canada (NSERC).

Model-based approaches try to build models that describe defect-free textures upon which defects can be compared and detected. For instance, an approach using Markov random fields (MRFs) has been proposed by Cohen et al. (1991) for defect inspection of fabrics. However, MRFs incur a huge computation time. Besides, selection of appropriate texture scale is not addressed by this approach. Recently, Sezer et al. (2007) have used independent component analysis (ICA) to detect defects at the bloc level in texture images. This approach has obtained good results in gray-level uniform textures. However, it does not generalize well to patterned textures, and several defects are not detected by this approach.

In this paper, we propose a novel defect detection algorithm which has the capability to cope with different types of defects and textile textures. Our algorithm is based on two phases. In the first phase, for each textile category, we use a set of training images of that category and label them at the block level as defected or containing no defects. That is, each training image is divided into a set of regular blocks from which we calculate statistical signatures based on mixtures of generalized Gaussian distributions (MoGG) (Allili et al. (2014)). In a nutshell, these signatures describe the distribution of contourlets coefficients at different scales and orientations of the image (Allili and Baaziz (2011); Baaziz (2005)). In each training image, distances are computed between signatures of a designated defect-free reference block and all blocks of the image. Using these distances, we train a binary Bayes classifier (BC) for discriminating defected and defect-free classes. In the inspection phase, new images are analyzed at the block level and classified using our trained BC model. Experiments conducted on the standard TILDA [1] database have shown that our algorithm outperforms most recent works in terms of accuracy and computation time.

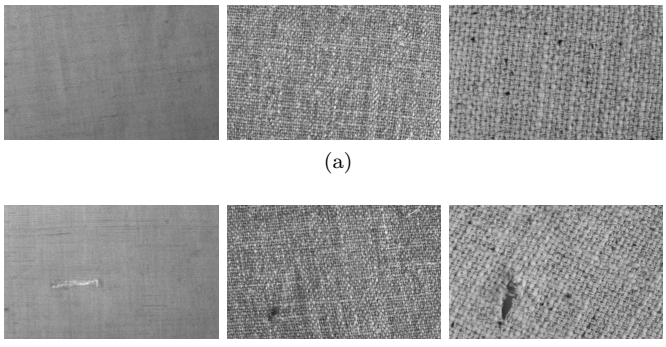

(a)

(b)

Fig. 1. Sample of images in the TILDA database: (a) without defects, (b) with defects

This paper is organized as follows: Section 2 presents a brief background theory for the standard and redundant contourlet transforms. Section 3 presents our method for defection detection. Section 4 presents some experimental results for our defect detection. We end the paper with a conclusion and future work perspectives.

[1] http://lmb.informatik.unifreiburg.de/resources/datasets /tilda.en.html.

2. STATISTICAL TEXTILE TEXTURE MODELING

2.1 The redundant contourlet transform

The standard contourlets transform (SCT) was introduced by Do and Vetterli (2002, 2005) to address the major limitation of the 2D discrete wavelet transform which are limited in their ability to capture directional information in natural images. the SCT has two distinct parts: a Laplacian pyramid (LP) decomposition to create levels of image resolution and directional subband decomposition using a bank of 2D filters. Each LP subband is split into different and flexible number of frequency wedge-shaped subbands allowing to capture geometric structures and directional information in images. These facts motivate the use of contourlets in the extraction of significant image features for texture analysis.

When cooperation between different contourlet subbands is required, it is desirable to have the subbands of the same size in order to avoid problems of interpolation and make easy correspondence between the different levels of resolution. For this goal, a new variant of SCT named the redundant contourlet transform (RCT) has been proposed (Baaziz (2005)). The RCT shares the same decomposition scheme with SCT. However, all down-sampling operations in the RCT are discarded from the Laplacian stage and a set of symmetric low-pass filters having adequate frequency selectivity and pseudo-Gaussian properties are employed. Filter impulse responses $g_b(n)$ are finite and symmetric, as given in Eq. (1), where b is a factor influencing the frequency bandwidth:

$$g_b(n) = e^{-2\frac{n}{b}} - e^{-2}\left(e^{-2(\frac{n-b}{b})^2} e^{-2(\frac{n+b}{b})^2}\right). \qquad (1)$$

Using L filters (with $b = 2, 4, 8, 16$) results into a redundant Laplacian pyramid (RLP) having $L+1$ equal-size sub-images: one coarse image approximation and L band-pass sub-images. Then, a DFB with $D = 4$ orientations and 1:4 critical down-sampling is applied on each of the L RLP subbands to obtain $4L$ equal-size directional subbands $(C_{ld}, l = 1, \ldots, L;\ d = 1, \ldots, D)$ in addition to a 1:4 down-sampled image approximation $C_L$as shown in Fig. 2.

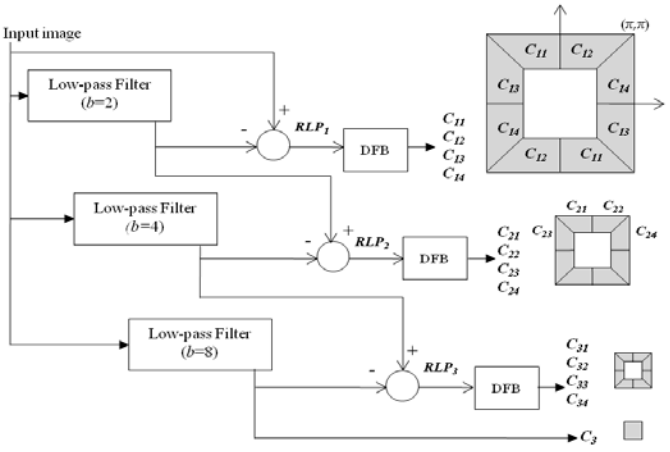

Fig. 2. Three level RCT decomposition scheme ($L = 3$) and corresponding frequency partition. No down-sampling operations are performed at the Laplacian stage

2.2 MoGG modeling of RCT coefficients

The general Gaussian distribution for a univariate random variable $\mathbf{x} \in \mathbb{R}$ is defined as follows:

$$p(x|\mu,\sigma,\beta) = \frac{\beta\sqrt{\frac{\Gamma(3/\beta)}{\Gamma(1/\beta)}}}{2\sigma\Gamma\left(1/\beta\right)}\exp\left(-A(\beta)\left|\frac{x-\mu}{\sigma}\right|^{\beta}\right), \quad (2)$$

where $A(\beta) = \left[\frac{\Gamma(3/\beta)}{\Gamma(1/\beta)}\right]^{\frac{\beta}{2}}$, $\Gamma(\cdot)$ denotes the gamma function. μ and σ are respectively the distribution mean and standard deviation parameters. The β is the flexible shape parameter which fits the kurtosis of the pdf and determines whether the distribution is peaked or flat. As $\beta \to \infty$ the distribution becomes uniform; whereas, when $\beta \to 0$, the distribution becomes a delta function with center at center at μ. As $\beta = 2$ the function becomes a Gaussian.

For multi-modal data, the marginal distribution of a random variable $\mathbf{x} \in \mathbb{R}$ is the resultant of a mixture of generalized Gaussian distributions (MoGG). Given a MoGG with K components, this is given by:

$$p(x|\Theta) = \sum_{i=1}^{K} \pi_i p(x|\mu_i,\sigma_i,\beta_i), \quad (3)$$

where $0 < \pi_i \leq 1$, $\sum_{i=1}^{K}\pi_i = 1$ and Θ denotes the set of model parameters $\{\pi_i, \mu_i, \sigma_i, \beta_i, i = 1,\ldots,K\}$. The model selection and parameter estimation of the MoGG is achieved in an unsupervised fashion using the minimum message length (MML) principle Wallace (2005). The MML provides a natural tradeoff between model complexity and goodness of fit for a given sample of data $\mathcal{X} = \{x_1, x_2, ..., x_n\}$. The details of parameter estimation of the MoGG are given in Allili et al. (2014).

2.3 Similarity measurement of RCT-MoGG signatures

Do and Vetterli (2005) have used a closed-form Kullback-Leibler divergence (KLD) to measure similarity between two statistical distributions of wavelet subband coefficients. When these distributions are multi-modal, a closed-form solution is intractable (Allili (2012)). To circumvent this issue, we resort to approximating the KLD using Monte-Carlo sampling methods, as proposed by Allili et al. (2014). Given two MoGG models $P(x) = \sum_{i=1}^{K}\pi_i p(x|\theta_i)$ et $Q(x) = \sum_{j=1}^{M}\omega_j q(x|\theta_j)$, the KLD between these models is defined as follows:

$$KLD(P||Q) = \int P(x)\log\left(\frac{P(x)}{Q(x)}\right)dx. \quad (4)$$

The KLD by Monte Carlo integration is given by:

$$KLD_{mc}(P||Q) = \frac{1}{n}\sum_{i=1}^{n}\log\frac{P(x_i)}{Q(x_i)} \approx_{n\to\infty} KLD(P||Q). \quad (5)$$

The approximation method by sampling aims to generate a sufficiently large sample $\mathcal{X} = \{x_1, x_2, ..., x_n\}$ drawn independently from P in order to approximate the KLD using the Monte Carlo integration (5).

3. PROPOSED ALGORITHM FOR DEFECT DETECTION

The flowchart of our algorithm is shown in Fig. 3. As mentioned previously, the defect detection process in our approach is divided into two phases: *a learning phase*, in which a classifier is trained on a set of training examples, and an *inspection phase*, which uses the trained classifier on a set of newly seen images to detect potential defects. Our algorithm operates at the block level of images which aims at localizing defects at fine resolutions allowed by the block decomposition.

3.1 The learning phase

Let $\mathcal{T} = \mathcal{B} \cup \tilde{\mathcal{B}}$ be the set of training examples composed of two subsets $\mathcal{B} = \{B_1, ..., B_n\}$ and $\tilde{\mathcal{B}} = \{\tilde{B}_1, ..., \tilde{B}_m\}$, containing defect-free and defective blocks, respectively. For each block in $\mathcal{T}$, we calculate its RCT-MoGG signature which combines several orientations and scales of the texture. The training process of the defect detection system is given by the script of Alg. 1. The algorithm trains a Bayes classifier BC and results into a set of reference blocks $\mathcal{R}$ that will be used to inspect newly-seen textile images. The set $\mathcal{R}$ is a sort of a landmark signature that contains the different configurations and patterns of the textile type to be inspected.

The training process iterates on the sets $\mathcal{B}$ and $\tilde{\mathcal{B}}$ by choosing at each time a new reference block to add to the set $\mathcal{R}$. The first reference block $B_{r_1} \in \mathcal{R}$ can be chosen randomly from $\mathcal{B}$. After calculating the KLDs of all the training blocks with B_{r_1}, we obtain the sets $\mathcal{D} = \{d_1, ..., d_n\}$ and $\tilde{\mathcal{D}} = \{\tilde{d}_1, ..., \tilde{d}_m\}$ for $\mathcal{B}$ and $\tilde{\mathcal{B}}$, respectively. Then, we train a Bayes classifier (BC) on $\mathcal{D} \cup \tilde{\mathcal{D}}$ where a Gaussian $P_{\mathcal{B}}$ (resp. $P_{\tilde{\mathcal{B}}}$) is fitted to class $\mathcal{B}$ (resp. $\tilde{\mathcal{B}}$). After classifying the training blocks using BC, we obtain the classification error ε (i.e., number of badly classified blocks) and the set $\mathcal{C}$ of false defect detections (i.e., blocks in $\mathcal{B}$ classified as defected by BC).

To augment the set $\mathcal{R}$ with a new reference block, we search for a block in $\mathcal{C}$ corresponding to either the median or the maximum of distances in $\mathcal{C}$. Using the new set $\mathcal{R}$, we update the distances $\mathcal{D}$ and $\tilde{\mathcal{D}}$ as follows. Let B_k be a block in $\mathcal{T}$ and $KLD_{r_1}, ..., KLD_{r_N}$ are the set of KLDs calculated with all reference blocks in $\mathcal{R}$, where N is the cardinality of $\mathcal{R}$. The new KLD assigned to the block for the next iteration (Step 2 of the algorithm) is given by $d_k = \min\{KLD_{r_1}, ..., KLD_{r_N}\}$ and a new BC is trained with the new sets $\mathcal{D}$ and $\tilde{\mathcal{D}}$. This process is repeated until the classification error ε is null or higher than ε_p, the classification error at previous iteration.

3.2 The inspection phase

The inspection phase is performed on a newly-seen textile image of the same type as the one used in the learning phase. The steps of the inspection process are given in the script of Alg. 2. First, the input textile image is decomposed into blocks with the same dimension as the training ones. Each block is then classified as containing defects or defect-free using the reference set $\mathcal{R}$ and the

Algorithm 1 Defect detection learning phase.

Data: $\mathcal{B} = \{B_1, ..., B_n\}$ and $\tilde{\mathcal{B}} = \{\tilde{B}_1, ..., \tilde{B}_m\}$.
Result: Set of reference blocks: $\mathcal{R}$, Bayes classifier: BC.
Generate RCT-MoGG signature for each block in $\mathcal{B}$ and $\tilde{\mathcal{B}}$

$\mathcal{R} \leftarrow B_1$; $\varepsilon \leftarrow \infty$; $\mathcal{C} \leftarrow \emptyset$; $N \leftarrow 0$;
repeat
1- $N \leftarrow N + 1$;
2- $\varepsilon_p \leftarrow \varepsilon$;
3- Update the set $\mathcal{R}$ from $\mathcal{C}$;
4- Calculate the KLDs $\{d_1, ..., d_n\}$ and $\{\tilde{d}_1, ..., \tilde{d}_m\}$;
5- Train a Bayes classifier on the calculated KLDs ;
6- Classify the KLDs and calculate the error ε;
7- Update $\mathcal{C}$ the set of false defect detections;
until ($\varepsilon = 0$ OR $\varepsilon \geq \varepsilon_p$)

trained Bayes classifier BC. Note that in order to achieve very precise localisation of defects, image subdivision into blocks may be performed with overlapping. For instance, if the block size is $W \times W$, and the overlapping between each block and its neighborhood is $W/2$, then the defect detection is done at the $W/2 \times W/2$ resolution level in the image, as illustrated in Fig. 4.

Algorithm 2 Inspection for defect detection.

Data: Input image I, $\mathcal{R} = \{B_{r_1}, ..., B_{r_N}\}$ and the Bayes classifier BC.
Result: Image with blocks classified.

Decompose the image into blocks;
Generate RCT-MoGG signature for each block;
for (each block B_k) **do**
1- Calculate the KLDs $\{KLD_{r_1}, ..., KLD_{r_N}\}$;
2- Choose $d_k = \min\{KLD_{r_1}, ..., KLD_{r_N}\}$;
3- Use BC to classify B_k as containing defects or defect-free.
end for

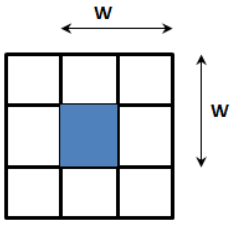

Fig. 4. Illustration of block overlapping in our defect detection method. Four blocks of size $W \times W$ participate to the decision making about the blue square of size $W/2 \times W/2$ at the middle.

4. EXPERIMENTAL RESULTS

In order to validate the proposed scheme for fabric defect detection, we conducted a sequence of tests on various texture images from the TILDA database which is a common benchmark for textile defect detection studies. TILDA database consists of four different groups (C1, ..., C4). Each group contains two textile types which are stored in seven defect classes (E1,. . . , E7) and one defect-free class (E0). Each class contains 50 images. For our study we were interested only in three types of textiles, namely, C1R1, C2R2 and C2R3. For each textile type, a learning set is composed from 30 images; six defect-free images from class E0 and 24 defective images containing various defects from classes E1 to E4. Based on image subdivision into overlapping blocks with size of 64 × 64 pixels, a ground truth is manually constructed for each of the three training sets. Table 1 shows obtained classification error values in the learning phase for the three studied types of textile. Given the error rate ε, calculated for each iteration in the learning phase, the best error rate is defined as $min(\varepsilon/(m+n))$, m and n being the number of defective and non-defective blocks used in this phase, respectively.

Table 1: Learning phase: Classification error statistics

Fabric type	C1R1	C2R2	C2R3
Nb of defective blocks (m)	782	292	531
Nb of non-defective blocks (n)	9568	10058	9819
Nb of iterations ($N+1$)	2	2	2
Classification error ε for each iteration	[289; 371]	[90; 268]	[171; 387]
Best error rate	2.79 %	0.86 %	1.65 %

One can observe in Table 1 some very good classification error rates ranging from 0.90% to 2.80% with the use of a single reference block. The inspection phase is performed on new textile images of the same type as the ones used in the learning phase. Figs. 5, 6 and 7 show some examples of our defect detection results compared to those obtained by the ICA reference method as described in Sezer et al. (2007), which we have implemented for a comparison purpose.

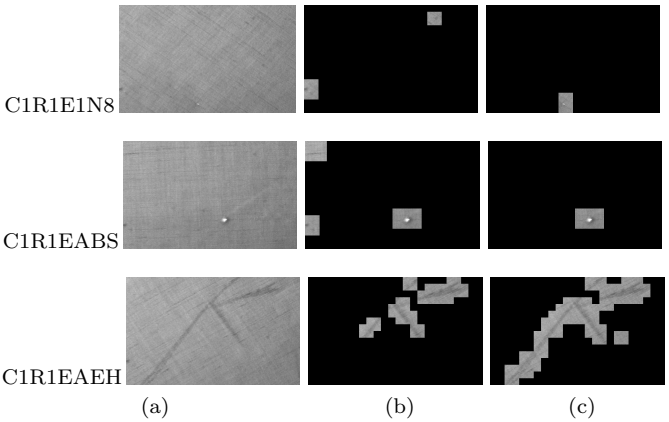

Fig. 5. Defect detection results for fabric type C1R1: (a) defective test images, (b) results from the ICA reference method, (c) our results

In Fig. 5, defect detection results for images C1R1E1N8 and C1R1EABS show that ICA reference method can fail and even generate false positive results (i.e., it detects defect free blocks as defective), while our method is more

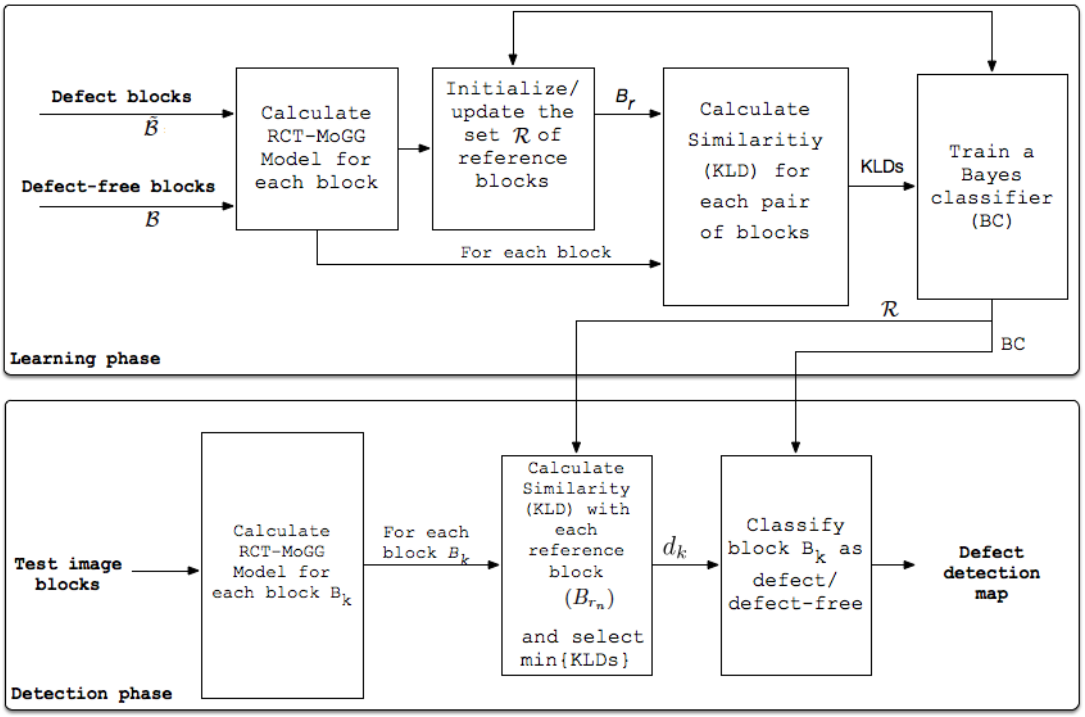

Fig. 3. Overall diagram of the proposed defect detection method according to Algorithms 1 and 2

successful. Furthermore, the results for C1R1EAEH image show that our method is able to detect almost all defective blocks in the image, so it is more accurate in detecting and localizing defective blocks. In Fig. 6 and 7, one can see that our method keeps the same high degree of reliability in detecting defects on both textile types C2R2 and C2R3, despite the poor regularity of the texture in those fabrics. Indeed, for both C2R2 and C2R3 textile types, there are some imperfections in their texture that are not regarded as defects but have been detected as defectives by the reference method, Whereas our method avoids these false alarms. Image C1R1E1N8 in Fig. 5 and images C2R2ECOC and C2R2E4N8 in Fig. 6 are good examples to illustrate this fact. Thanks to the RCT-MoGG signatures, our algorithm has been able to classify very precisely image blocks containing defects with mild imperfections.

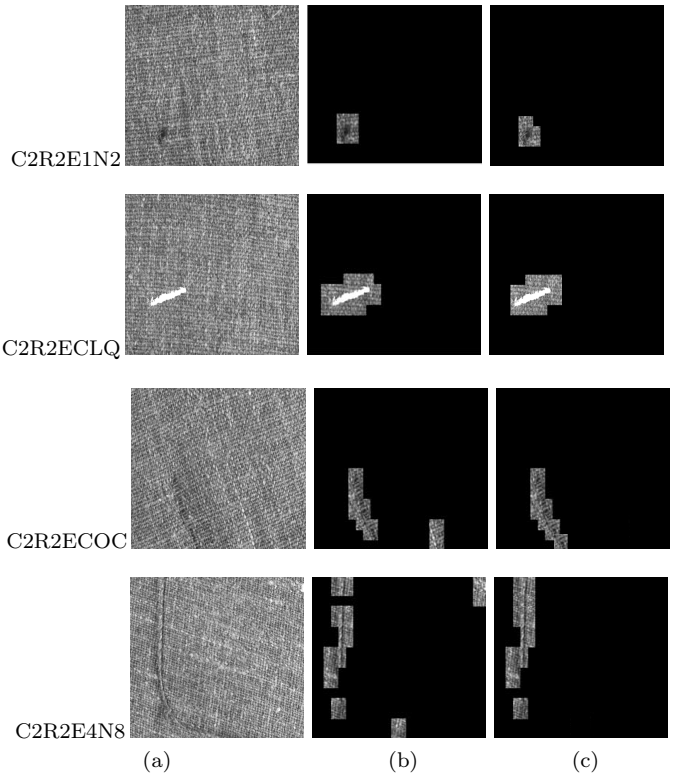

Fig. 5. Defect detection results for fabric type C2R2: (a) defective test images, (b) results from the ICA reference method, (c) our results

5. CONCLUSION

We have presented a new textile defect detection method based on a statistical and multi-resolution modeling of texture images combined with a naive Bayes classification. In comparison to the ICA-based reference approach, our method gave more accurate results, and notably showed its efficiency in separating defect-free from defective areas of the texture. This augmented precision is of crucial for textile industry, as automatic quality control may play an important role for augmenting productively. In the future, we will focus on developing multi-channel signatures for defect detection in color textures as well as applying our approach for other fabric materials.

REFERENCES

Allili, M. (2012). Wavelet modelling using finite mixtures of generalized gaussian distributions: Application to

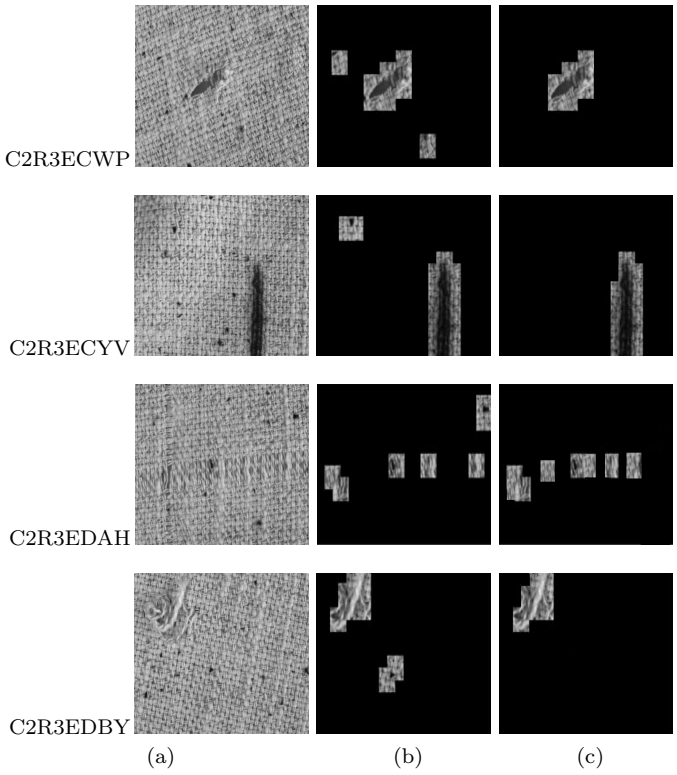

Fig. 6. Defect detection results for fabric type C2R3: (a) defective test images, (b) results from the ICA reference method, (c) our results

texture discrimination and retrieval. *IEEE Trans. on Image Processing*, 12(4), 1452–1464.

Allili, M. and Baaziz, N. (2011). Contourlet-based texture retrieval using a mixture of generalized gaussian distributions. *Computer Analysis of Images and Patterns*, 446–454.

Allili, M., Baaziz, N., and Mejri, M. (2014). Texture modeling using contourlets and finite mixtures of generalized gaussian distributions and applications. *IEEE Trans. on Multimedia*, 16(3), 772–784.

Baaziz, N. (2005). Adaptive watermarking schemes based on a redundant contourlet transform. *IEEE Int'l Conf. on Image Processing*, 221–224.

Chan, C. and Pang, G.K. (2000). Fabric defect detection by fourier analysis. *IEEE Trans. on Industry Applications*, 36(5), 1267–1276.

Cho, C., Chung, B., and Park, M. (2005). Development of real-time vision-based fabric inspection system. *IEEE Trans. on Industrial Electronics*, 52(4), 1073–1079.

Cohen, F., Fan, Z., and Attali, S. (1991). Automated inspection of textile fabrics using textural models. *IEEE Trans. on Pattern Analysis and Machine Intelligence*, 13(8), 803–808.

Do, M.N. and Vetterli, M. (2002). Contourlets : A directional multiresolution image representation. *IEEE Int'l Conf. on Image Processing*, 1, 357–360.

Do, M.N. and Vetterli, M. (2005). The contourlet transform: An efficient directional multiresolution image representation. *IEEE Trans. on Image Processing*, 14(12), 2091–106.

Kumar, A. (2008). Computer-vision-based fabric defect detection: A survey. *IEEE Trans. on Industrial Electronics*, 55(1), 348–363.

Kumar, A. and Pang, G. (2002). Defect detection in textured materials using gabor filters. *IEEE Trans. on Industry Applications*, 38(2), 425–440.

Ngan, H., G.H., Pang, Yung, S., and Ng, M. (2005). Wavelet based methods on patterned fabric defect detection. *Pattern Recognition*, 38(4), 559–576.

Ngana, H., Panga, G., and Yung, N. (2011). Automated fabric defect detectiona review. *Image and Vision Computing*, 29(7), 442–458.

Sezer, O., Ertuzun, A., and Ercil, A. (2007). Using perceptual relation of regularity and anisotropy in the texture with independent component model for defect detection. *Pattern Recognition*, 40(1), 121–133.

Tajeripour, F., Kabir, E., and Sheikhi, A. (2008). Fabric defect detection using modified local binary patterns. *EURASIP J. on Advances in Signal Processing*, ID 783898.

Wallace, C. (2005). Statistical and inductive inference by minimum message length. Information science and statistics. *New York. Springer, Heidelberg.*